TESTING OF DIODE-CLAMPING IN AN INDUCTIVE PULSED PLASMA THRUSTER CIRCUIT

Alexandra Toftul[1], Kurt A. Polzin[2], and Adam K. Martin[3]
NASA – George C. Marsahll Space Flight Center, Huntsville, AL 35812

and

Jerry L. Hudgins[4]
University of Nebraska-Lincoln, Lincoln, NE 68588

Testing of a 5.5 kV silicon (Si) diode and 5.8 kV prototype silicon carbide (SiC) diode in an inductive pulsed plasma thruster (IPPT) circuit was performed to obtain a comparison of the resulting circuit recapture efficiency, η_r, defined as the percentage of the initial charge energy remaining on the capacitor bank after the diode interrupts the current. The diode was placed in a pulsed circuit in series with a silicon controlled rectifier (SCR) switch, and the voltages across different components and current waveforms were collected over a range of capacitor charge voltages. Reverse recovery parameters, including turn-off time and peak reverse recovery current, were measured and capacitor voltage waveforms were used to determine the recapture efficiency for each case. The Si fast recovery diode in the circuit was shown to yield a recapture efficiency of up to 20% for the conditions tested, while the SiC diode further increased recapture efficiency to nearly 30%. The data presented show that fast recovery diodes operate on a timescale that permits them to clamp the discharge quickly after the first half cycle, supporting the idea that diode-clamping in IPPT circuit reduces energy dissipation that occurs after the first half cycle.

Nomenclature

C	=	capacitance
E_{Ci}	=	initial capacitor energy
E_{Cf}	=	final capacitor energy
$i(t)$	=	loop current
I_{dRM}	=	peak reverse recovery current
$I_{F,AV}$	=	mean forward current
Q_{rr}	=	reverse recovery charge
t_o	=	time of initial current zero crossing
t_{rr}	=	reverse recovery time
$V_C(t)$	=	capacitor voltage
V_{Ci}	=	initial capacitor voltage
V_{Cf}	=	final capacitor voltage
V_{RRM}	=	maximum reverse blocking voltage
z_o	=	electromagnetic decoupling distance
η_r	=	recapture efficiency

[1] Flight Systems Engineer, Systems Integration Branch, Vehicle Integration Depatment, alexandra.toftul@nasa.gov, Member AIAA.
[2] Propulsion Research Scientist, Propulsion Research and Technology Applications Branch, Propulsion Systems Department, kurt.a.polzin@nasa.gov, Associate Fellow AIAA
[3] Physicist, Propulsion Research and Technology Applications Branch, Propulsion Systems Department, adam.k.martin@nasa.gov
[4] Professor and Chair, Department of Electrical Engineering, jhudgins2@unl.edu

I. Introduction

INDUCTIVE pulsed plasma thruster (IPPT) circuits, such as those needed to operate the Pulsed Inductive Thruster (PIT), are required to quickly switch high-voltage capacitor banks through an inductive acceleration coil at current levels on the order of at least 10 kA operating on a period of 1-10 μs.[1] In most IPPTs, the required voltage holdoff between pulses and the high current levels during pulses have led to the use of spark gaps in discharging the capacitor bank. Recent availability of fast solid-state switching devices capable of both holding off high voltages and conducting increasingly high current has made it possible to consider the use of these switches in modern IPPTs. In addition, the production of a pre-ionized gas prior to the discharge through the acceleration coil permit a reduction in the required discharge energy per pulse for electric thrusters of this type, relaxing the switching requirements for these thrusters.[2] Solid state switches offer the advantage of greater controllability, reliability, and longer lifetime, as well as decreased drive circuit dimensions and mass relative to spark gap switches.

The capacitor bank, inductive acceleration coil, and external resistance and inductance of an IPPT pulse circuit can be modeled as a simple series resistive-inductive-capacitive (*RLC*) circuit. Once the switch is closed, the natural energy exchange between the reactive components will cause the stored energy in the circuit to oscillate between the capacitive and inductive elements until it has been used to accelerate a plasma or resistively dissipated in the circuit. It has been previously shown[3,4,5] that the most efficient coupling of energy into the plasma current sheet of a PIT occurs during the first current half-cycle of the capacitor discharge, when the coil current and current rise rate are maximum and the plasma is spatially closest to the coil. After this time, the current sheet has moved away and is largely electromagnetically decoupled from the inductive coil, leaving the remaining energy in the circuit to be resistively dissipated while performing no work. This energy could be recaptured in the capacitor bank and used in-part for future pulses if the current flow in the circuit can be interrupted after the first half-cycle of the discharge.

Energy recapture can be achieved by placing a fast turn-off diode in series with the main switch. In this case, higher circuit recapture efficiency, η_r, defined as the percentage of the initial charge energy remaining in the capacitor bank after current stops flowing, may be achieved by using a diode that is able to transition, or 'switch,' from the forward conducting state ('on' state) to the reverse blocking state ('off' state) in the shortest amount of time, minimizing current ringing and switching losses. This is known as the reverse recovery time and is dependent on the diode material and internal structure. Investigating the effect of diode reverse recovery on recapture efficiency could potentially lead to the development of novel, high-efficiency IPPT circuit topologies.

In Section II, we describe the motivation for more efficient utilization of electrical energy in IPPT pulse circuits and propose how this can be improved through the use of fast recovery diodes (FRDs). Described in Section III is the design and fabrication of the small-scale IPPT used as a testbed for the several types of diodes. In Section IV, we present the experimental setup used to test several different diode types and quantify their ability to interrupt the oscillating current in the pulse circuit. Comparative data demonstrating the capability to clamp the circuit with different types of diodes, recapturing otherwise dissipated energy in the capacitor bank, are presented in Section V.

II. Inductive Pulsed Plasma Thruster Circuit Topology

After an IPPT completes the first half-cycle of the discharge, during which inductive acceleration of a plasma occurs, any further oscillation of the discharge current causes excess heat generation and power waste, both of which are highly undesirable in a space environment. In the absence of convective cooling, heat removal from circuit components becomes a major concern, particular for electrical components that may fail above a maximum rated operating temperature that is still quite low in terms of the ability to radiate that energy to space. Heating must be managed using heat sinks, which can add significant mass to a system. Similarly, inefficient use of electrical energy necessitates a larger, more massive, and typically more costly electrical power system (EPS). Furthermore, voltage reversals in the circuit have been shown to adversely affect capacitor lifetime.[6] In the absence of a snubber circuit, the high reverse voltage rise rate can stress the solid state switch, reducing the long-term reliability of the device. As IPPTs are designed for long-duration, deep-space missions that may require the pulse circuit to survive for upto 10^{10} discharge cycles[7], these reductions in component reliability and lifetime are problematic. While the use of one or more redundant circuits will reduce the probability of a system failure, the associated increase in thruster mass, volume, cost, and complexity are clearly undesirable.

To address these issues, a FRD can be placed in series with an IPPT's switch. The purpose of the diode is to clamp the current in the circuit following the first half-cycle of the discharge. Two PiN structure power diodes[8] were tested in the circuit in Fig. 1 to determine the effect of the diode material on the IPPT circuit recapture efficiency, η_r. The two series diodes tested were a silicon (Si) ABB 5SDF 02D6004 PiN power diode rated for 5.5 kV and 175 A (Fig. 2a), and a prototype silicon carbide (SiC) PiN diode from Cree, Inc. rated at 5.8 kV (Fig. 2b). While a current rating for the prototype device is not available, thermal analysis suggests that the device can withstand currents in a 10 μs pulse of up to 400 A. The diode is placed in series with an SCR switch, which is a Dynex™ PT85QWx45, optimized for pulsed power applications. The switch is rated for a maximum reverse blocking voltage, V_{RRM}, of 4.5 kV and a mean forward current, $I_{F,AV}$ of 1670 A. Connecting each diode into the circuit in the same manner yields the same circuit losses for each diode, including conduction and switching losses of the main switch and FRD. This makes the recapture efficiency our best metric for an equivalent, quantitative comparison between the two diodes.

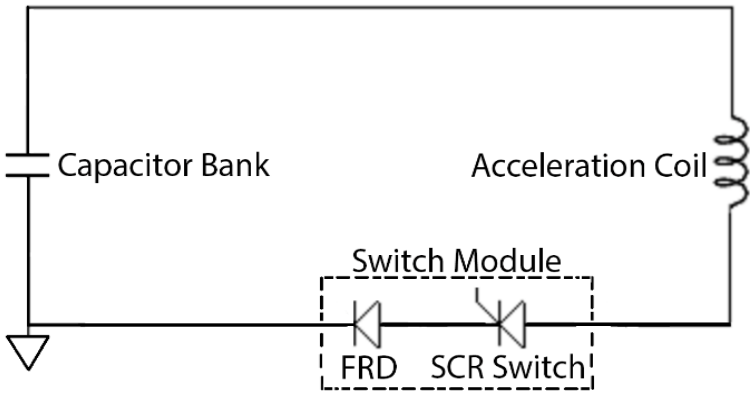

Figure 1. Simplified IPPT circuit schematic showing the circuit with a series SCR switch and FRD.

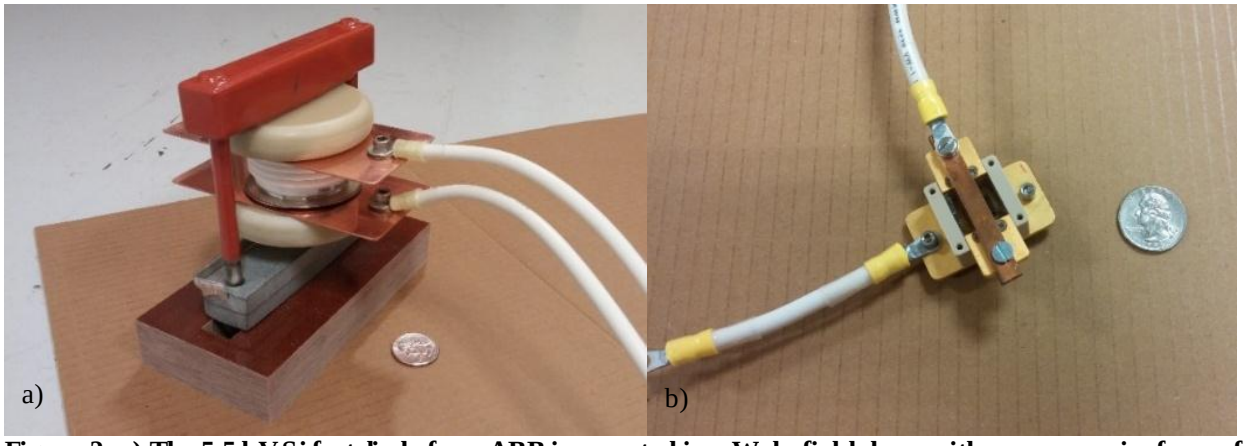

Figure 2. a) The 5.5 kV Si fast diode from ABB is mounted in a Wakefield clamp with a compressive force of approximately 16 kN. b) A 5.8 kV SiC PiN diode from Cree, Inc.

In other applications, it has been shown[9] that SiC devices have a superior reverse recovery response as compared with similarly rated Si devices. The wider bandgap of the material results in a breakdown voltage 10 times higher than that of Si,[10] making it an ideal material for high voltage applications. In addition, the non-linear relationship between the drift region thickness and breakdown voltage allows for much thinner drift regions in wide bandgap devices, resulting in lower conduction voltage drop[11,12] and less time needed for reverse recovery due to a lower volume of excess charge carriers. SiC also has a high thermal conductivity as compared to other semiconductor materials, and can therefore operate at higher temperatures. Further information on the SiC material properties and its subsequent incorporation into solid-state device designs can be found in Ref. 11. These characteristics make SiC devices highly promising for IPPT applications as we might expect a SiC diode to result in higher circuit recapture efficiency than what can be obtained using a conventional Si diode. However, SiC device manufacturing is a relatively new process[13], and validation testing must be performed to determine how they will perform in high-power pulsed circuit applications.

III. Testbed Thruster Design and Construction

A modular, small-scale IPPT was designed and fabricated at NASA Marshall Space Flight Center (MSFC) to serve as a flexible testbed for solid state switching components and pulsed propellant injection technologies. As these components are integrated and tested in the device, it will eventually permit testing in repetition-rate mode, as opposed to the single-shot testing that has historically been completed in other IPPT development projects.[14] Thruster design specifications and main subsystem fabrication for the bench-top testing configuration are discussed in the following section. Additional information on the testbed thruster design and fabrication can be found in Ref. 14.

The testbed thruster was fabricated using a combination of custom and commercial off-the-shelf (COTS) components. Of the five major subsystems, only three are assembled and integrated for the preliminary bench-top testing described in this paper. These are the acceleration coil, the capacitor bank, and the switch module. A preionizer and pulsed propellant injection valve are not necessary for the electrical switching tests and were not installed for the present work. The thruster electrical parameters are summarized in Table 1.

Table 1. Testbed thruster electrical circuit parameters.

Electrical Parameter	Nominal Value
Energy, J/pulse	80
Pulse Length, μs	~20
Charge Voltage, kV	Up to 4
Peak Coil Current, kA	>12
Capacitor Bank, μF	Selectable: 10, 20, or 30 μF
Coil Inductance, nH	650
Circuit Stray Inductance, nH	200
Predicted Circuit Stray Resistance, mΩ	10
Switch Type	Silicon-controlled rectifier

The primary materials used in the prototype testbed fabrication are Lexan, phenolic, and fiberglass rod. A Lexan frame provides the structure on which all thruster components are mounted. The frame is approximately 40 cm (15.75 in) wide, 40 cm (15.75 in) tall, and 38 cm (15 in) long. Four 35 cm (13.8 in) long, 1.6 cm (0.63 in) diameter fiberglass threaded rods connect the two separate pieces of 1.3-cm (0.5 in) thick Lexan that constitute the frame. Components are then mounted onto the rods to hold everything together.

A. Acceleration Coil

The acceleration coil, shown in Fig. 3, consists of six 10 gauge copper coil wire leads connected in parallel to the remainder of the pulse circuit. The flat coil geometry was chosen because it is relatively simple to fabricate and has been used for previous IPPTs, including the PIT and the Faraday Accelerator with Radio-frequency Assisted Discharge (FARAD) thrusters.[1,2,14] The copper coil leads are placed in grooves machined in a Lexan coil form, where each path is in the form of an Archimedes spiral. The inner diameter of the coil is 5 cm (2 in), and the outer diameter is 15 cm (6 in). Each lead starts on the front side of the Lexan coil form, spirals radially outward toward the edge of the pattern, passes through a hole in the Lexan to the back side of the coil, and then spirals radially inward to a point on the backside that is directly opposite from its starting point.

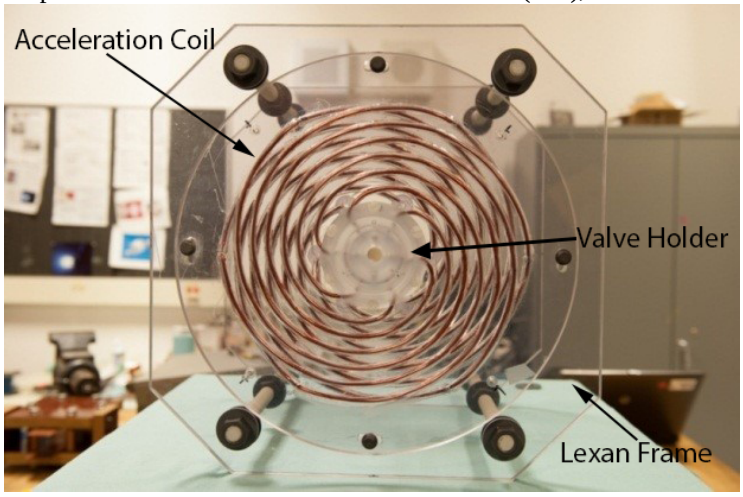

Figure 3. Photograph of the testbed thruster acceleration coil.

During actual thruster operation, the mutual inductance between the acceleration coil and the plasma current sheet varies as the plasma is accelerated away from the coil. However, in the present work data are presented only for the electrical circuit parameters corresponding to the case where the "plasma" is infinitely far from the coil face. Practically speaking, the plasma is at a

distance much greater than the coil's electromagnetic decoupling distance, z_o, such that the mutual inductance between the coil and plasma currents has reduced to zero. The coil inductance, L_c, was measured as approximately 700 nH. For completeness, the decoupling distance for the coil, z_o is approximately 6 cm.

B. Capacitor Bank

Energy is stored in a capacitor bank (Fig. 4) and then discharged rapidly through the acceleration coil. The capacitor bank consists of three oil-filled, vacuum-compatible capacitors manufactured by CSI Capacitors. The total capacitance of the bank can be approximately 10, 20, or 30 µF, depending on how many of the capacitors are connected in parallel. For the bench-top testing described here, only one 10 µF was used. The measured capacitance was approximately 9.88 µF.

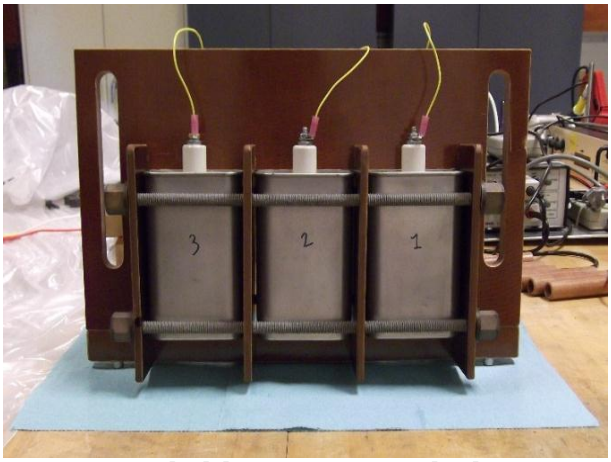

Figure 4. Testbed thruster capacitor bank.

C. Switch Module

The switch module was assembled in several configurations to permit a comparison of the turn-off, or circuit clamping, capability of two different power diodes to each other, and also to a baseline, no-diode configuration. The ceramic compression ("hockey puck") package SCR is clamped with an applied force of 40 kN (± 10%). The mounting yoke that is used to clamp the SCR consists of two 2.54-cm (1-in) thick phenolic slabs held together by six 13.97-cm (5.5 in) long stainless steel bolts. Phenolic tubes are used to electrically insulate the bolts (Fig. 5). To facilitate tightening of the bolts, sockets are welded to a metal plate to hold the module in place as the bolts were tightened with a torque wrench to the necessary compressive load. The thruster circuit stray inductance and series diode serve to limit the current and voltage rise rate through the SCR during switching, eliminating the need for a protective snubber circuit. The diodes are connected to the copper tabs clamped to either side of the SCR.

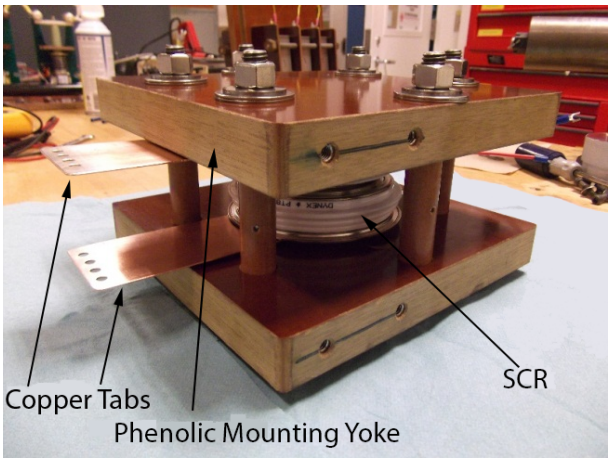

Figure 5. Assembled SCR switch module.

IV. Experiment

The assembled testbed thruster is shown in Fig. 6. Switching waveform measurements were recorded with no series diode in the circuit to obtain baseline unclamped waveforms. The measurement was repeated using one Si diode and two separate SiC diodes, in turn. Two SiC diodes of the same type were tested to determine whether performance was consistent between the two prototype devices. The circuit schematics and measurement locations for the testing are shown in Figs. 7a and 7b. The loop current is measured using a Pearson current monitor and the voltages across the switch and diode are measured using Tektronix differential high voltage probes. The SCR is activated by a 20 µs trigger pulse applied to the gate using a custom driver circuit.

The current and voltage waveforms collected for a switch module configuration containing only the Dynex SCR with no series FRD provide a baseline against which to evaluate the performance of the Si and SiC diodes in the IPPT. To minimize the risk of damaging the SCR with no diode protection from a high reverse voltage rise rate in place, the circuit in this configuration was operated at a relatively low charge voltage. The collected loop current and switch voltage waveforms for a nominal charge voltage of 250 V are shown in Figure 8a, while the capacitor voltage, $V_C(t)$, is shown in Figure 8b. The measured loop current $i(t)$ is used to calculate $V_C(t)$ as

$$V_C(t) = -\frac{1}{C}\int_0^t i(t)dt + V_{Ci} \quad (1)$$

where C is the capacitance and V_{Ci} is the initial capacitor charge voltage. We observe that the SCR conducts even after the initial current zero crossing, and does not permanently return to a blocking state after the 20 μs trigger pulse is removed. This implieds self-triggering of the SCR, likely caused by high values of reverse votage rise rate in the absence of the series FRD. A curvefit of the loop current waveform indicates a total circuit inductance and resistance of approximately 1.24 μH and 58.6 mΩ, respectively. The frequency of the waveform is found to be slightly greater than 45 kHz. For an unclamped configuration with no series FRD, all or nealy all voltage is assumed to be removed from the capacitor bank following a single ringing discharge cycle. In this case, η_r will be very small or zero.

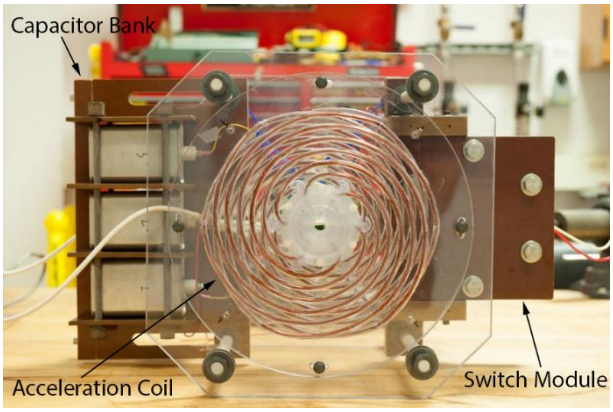

Figure 6. Assembled testbed thruster showing the acceleration coil, capacitor bank, and switch module.

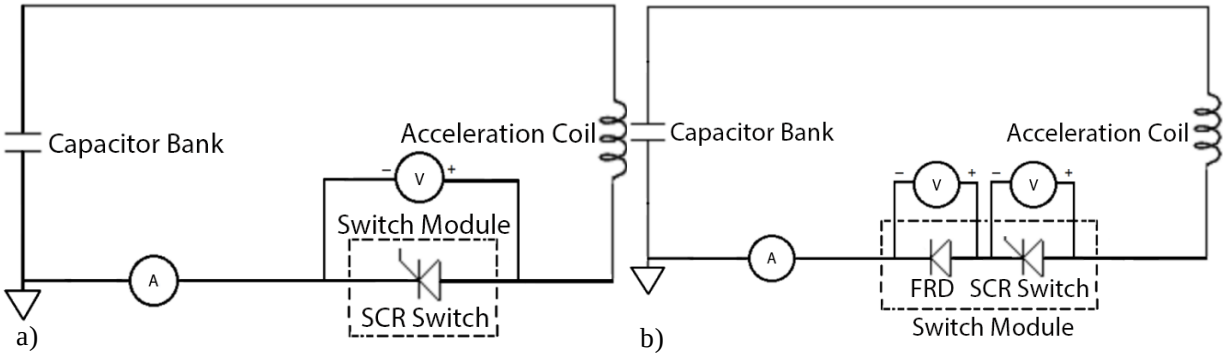

Figure 7. IPPT circuit configurations tested: a) Baseline no-diode configuration. b) Circuit configuration used to test the Si and SiC FRDs.

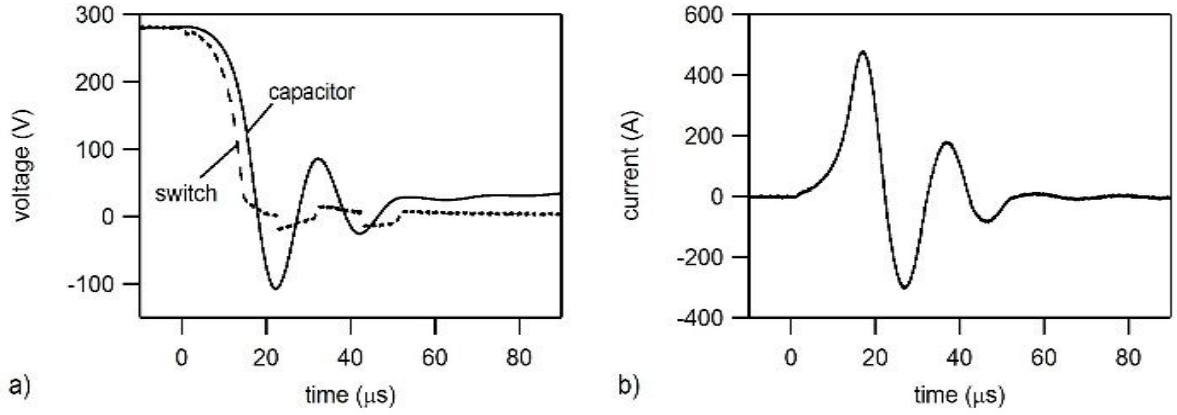

Figure 8. Baseline configuration waveforms at a nominal charge voltage of 250 V: a) measured switch voltage and calculated capacitor voltage and (b) loop current..

Switch voltage and loop current waveforms are collected for the Si diode and two SiC diodes of the same type. Measurements of both SiC diodes yielded very similar results, so only the waveforms for one are presented. Figure 9 shows a comparison between the calculated capacitor voltage and loop current for the Si and SiC diode configurations at a nominal charge voltage of 550 V.

The reverse recovery response is observed in the loop current waveform following the first zero corssing. A zoomed-in view of the reverse recovery waveforms (Fig. 9c) clearly shows that the SiC diode experiences a shorter

reverse recovery time and lower magnitude reverse recovery current than the Si diode. This relationship is found to hold for each charge voltage tested, as well as for the second SiC diode.

A. Recapture Efficiency

The capacitor voltage waveforms for the Si and SiC diodes, corresponding to nominal charge voltages of 300 V, 350 V, 450 V, and 550 V, are used to calculate the percent recapture efficiency as

$$\eta_r = \frac{E_{Cf}}{E_{Ci}} \times 100\% \tag{2}$$

where E_{Ci} and E_{Cf} represent the initial and final capacitor bank energies, respectively. These are calculated as

$$E_{Ci} = {}^1\!/_2\, C V_{ci}{}^2 \tag{3a}$$

and

$$E_{Cf} = {}^1\!/_2 C V_{cf}{}^2 \tag{3b}$$

where C denotes the capacitance and V_{Ci} and V_{Cf} are initial and final capacitor bank voltages. The recapture efficiencies for each circuit configuration are summarized in Table 2.

B. Diode Reverse Recovery

From the measured waveforms, it is apparent that there is a significant difference between the reverse recovery response of the Si and SiC diodes. The diode turn-off time is critical to the performance of the clamped IPPT circuit topology. For each diode, the magnitude of the reverse recovery response increases with increasing forward current. This is due to the greater amount of charge in the intrinsic region at turn-off.[12] The turn-off response can be quantified by computing the reverse recovery parameters, including peak reverse current, I_{dRM}, reverse recovery time, t_{rr}, and total reverse recovery charge, Q_{rr}. These are estimated from the reverse recovery waveform using a triangular appoxiamtion of the reverse current area (Fig. 10). Time t_o represents the time of the initial current zero crossing, while t_{rr} is the total time necessary for the diode to transition from a conduction state to a blocking state. The magnitude of I_{dRM} indicates the maximum reverse current seen by the device during turn-off. The triangular approximation calculates the total Q_{rr} as the area of the shaded region, where I_{dRM} estimates the height of the triangle and t_{rr} estimates the length of the base.

The total diode Q_{rr} is an important measure of the device turn-off time, in that the greater the charge stored in the intrinsic region at turn-off, the more time is necessary for the diode to transition from a conduction state to a forward blocking state. The charge must either be swept out of the region by an electric field, or recombine with other charged particles in the material. Longer turn-off time often implies high switching power losses and stress on circuit components. The parameters for all three diodes are tabulated in Table 3.

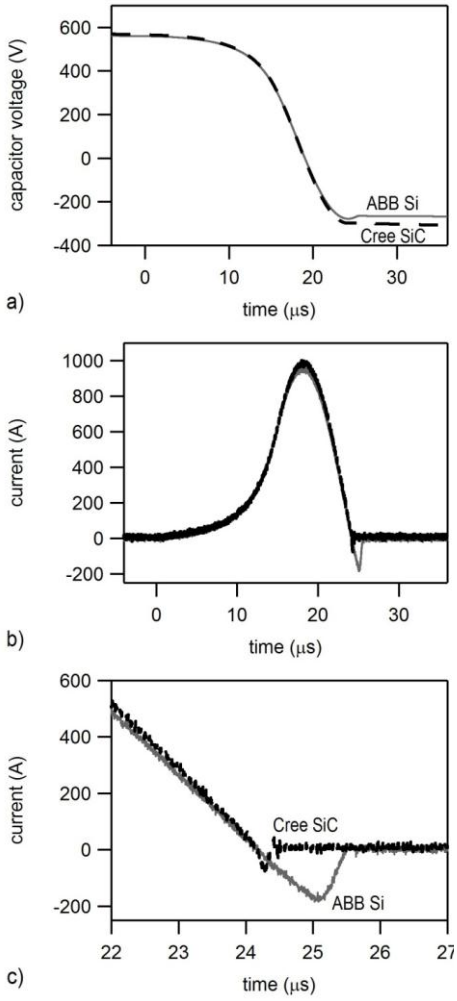

Figure 9. Comparison data collected for Si and SiC FRDs: a) calculated capacitor voltages, b) complete time-history of the loop currents, c) A zoomed-in view of current at reversal.

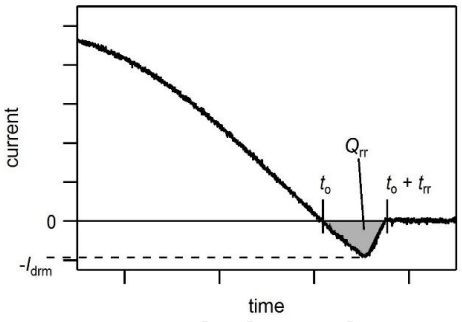

Figure 10. Graph showing how reverse recoevery parameters are defined.

Table 2. Tabulated test conditions and recapture efficiencies for the ABB Si diode and the two Cree SiC diodes.

Device Under Test	*Nominal Charge Voltage (V)*	*Initial Capacitor Energy, J*	*Final Capacitor Energy, J*	*Recapture Efficiency, %*
ABB Si	*300*	0.399	0.040	10.025%
	350	0.630	0.070	11.111%
	450	1.10	0.200	18.182%
	550	1.55	0.350	22.581%
Cree SiC 1	*300*	0.380	0.080	21.053%
	350	0.590	0.123	20.847%
	450	1.08	0.270	25.000%
	550	1.59	0.460	28.931%
Cree SiC 2	*300*	0.3902	0.060	15.312%
	350	0.6402	0.092	14.420%
	450	1.1093	0.237	21.405%
	550	1.5260	0.423	27.739%

Table 3. Tabluated reverse recovery parameters for the ABB Si diode and the two Cree SiC diodes.

Device Under Test	*Nominal Charge Voltage (V)*	I_{dRM}, A	t_{rr}, µs	Q_{rr}, µC
ABB Si	*300*	88.22	1.66	73.22
	350	105.5	1.55	81.76
	450	139.0	1.41	98.00
	550	172.0	1.32	113.52
Cree SiC 1	*300*	29.7	0.20	2.97
	350	42.5	0.25	5.31
	450	56.0	0.21	5.88
	550	64.0	0.21	6.56
Cree SiC 2	*300*	34.2	0.27	4.62
	350	39.8	0.24	4.77
	450	52.4	0.24	6.29
	550	65.8	0.24	7.89

The effect of the FRD on the IPPT circuit performance is evident in Fig. 11, which shows a comparison between the capacitor voltage and loop current waveforms for the no-diode, Si diode, and SiC diode configurations. Clamping of the circuit energy is observed in Fig. 11a, where both diodes serve to preclude ringing. Figure 11b highlights the difference between the current reversal for each configuration.

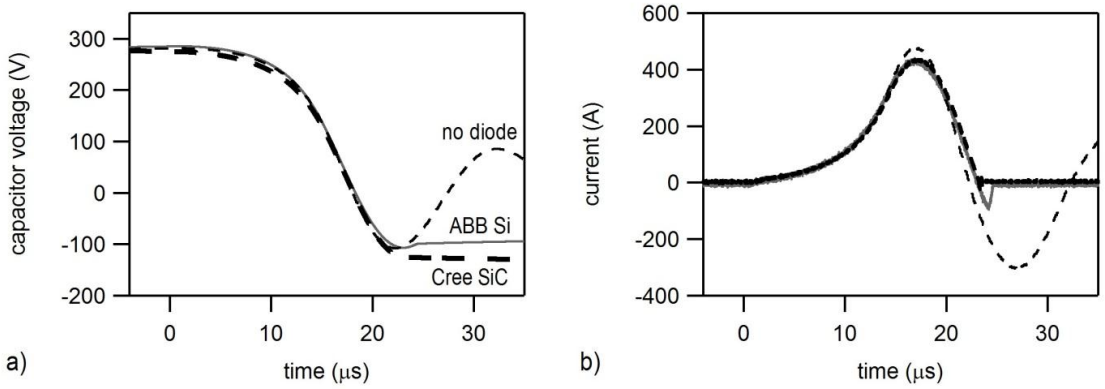

Figure 11. Comparison of waveforms at 250 V charge voltage for the no-diode, Si diode, and SiC diode configurations.

VI. Conclusion

The data demonstrate that diode-clamping in an IPPT circuit permits energy recovery by halting the discharge after the first half-cycle, limiting resistive dissipation and leaving the capacitor bank partially charged. This has the potential to make the circuit more energy efficient and can reduce heating through lower resistive dissipation. Both of these are significant advantages in a space environment, where the production of electricity can be costly from both a financial and mass allocation standpoint and where thermal management of power electronics is a serious concern. In addition, the comparison of the Si and SiC FRDs points to a significant advantage in using fast-switching SiC devices for this application. This point is quantified by the circuit recapture efficiency. The use of a series Si FRD in the drive circuit results in a maximum recapture efficiency of over 20% for the conditions tested, while the use of a SiC FRD results in a maximum recapture efficiency approaching 30%. The data show that this difference is largely due to the superior reverse recovery response of the SiC devices, which stems from the unique material properties of the wide bandgap material used.

Acknowledgments

The authors would like to acknowledge the management support of Mr. Jim Martin, Ms. Mary Beth Koelbl, Mr. Chad Summers, and Ms. Jeri Law. In addition, we appreciate the contributions and support of our colleagues Dr. Richard Eskridge, Darren Boyd, Doug Galloway, Tommy Reid, and Adam Kimberlin.

References

[1] Dailey, C. L., and Lovberg, R.H., "The PIT MkV Pulsed Inductive Thruster," NASA CR-191155, 1993.

[2]Polzin, K. A. "Faraday Accelerator with Radio-Frequency Assisted Discharge (FARAD)," Ph.D. Dissertation, Mechanical and Aerospace Engineering Dept., Princeton Univ., Princeton, NJ, 2006.

[3]Polzin, K. A., and Choueiri, Edgar Y., "Performance Optimization Criteria for Pulsed Inductive Plasma Acceleration," *IEEE Transactions on Plasma Science*, vol.34, no.3, pp.945,953, June 2006

[4]J. Bernardes, and S. Merryman, "Parameter analysis of a single stage induction mass driver," *5th IEEE International Pulsed Power Conference*, IEEE Paper PI-27, pp. 552-555, 1985.

[5]Dailey, C. L., and Lovberg, R.H., "Pulsed Inductive Thruster (PIT) Clamped Discharge Evaluation," TRW Applied Technology Div., Redondo Beach, CA, Rep. AFOSR-TR-89-0130, 1988.

[6]General Atomics Energy Products, "The Effect of Reversal on Capacitor Life," Engineering Bulletin 96-004, 2003.

[7]Polzin, K. A., "Comprehensive Review of Planar Pulsed Inductive Plasma Thruster Research and Technology," *Journal of Propulsion and Power*, Vol. 27, No. 3, pp. 513-531, 2011.

[8]Gustaveo, B., "Modeling and Simulation of Power PiN Diodes within SPICE," Ph.D. Dissertation, Electrical Engineering Dept., Polytechnic Univ. of Turin, Turin, Italy, 2006.

[9]Elasser, A., Agamy, M., Nasadoski, J., Bolotnikov, A., Stum, Z., Raju, R., Stevanovic, L., Mari, J., Menzel, M., Bastien, B., and Losee, P., "Static and Dynamic Characterization of 6.5kV, 100A SiC Bipolar PiN Diode Modules," *Energy Conversion Congress and Exposition (ECCE)*, 2012 IEEE, vol., no., pp.3595-3602, 15-20 Sept. 2012.

[10]Yu, L., "Simulation, Modeling, and Characterization of SiC Devices," Ph.D. Dissertation, Electrical and Computer Engineering Dept, Rutgers, The State Univ. of New Jersey, New Brunswick, NJ, 2010.

[11]Matsukawa, T., Chikaraishi, H., Sato, Y., and Shimada, R., "Basic Study on Conductive Characteristics of SiC Power Device for its Application to AC/DC Converter," *Applied Superconductivity, IEEE Transactions on*, vol.14, no.2, pp.690,692, June 2004

[12]Ostling, M., Ghandi, R., and Zetterling, C. -M, "SiC Power Devices — Present Status, Applications and Future Perspective," *Power Semiconductor Devices and ICs (ISPSD), 2011 IEEE 23rd International Symposium on* , vol., no., pp.10,15, 23-26 May 2011

[13]Matsunami, H., "Progress in Wide Bandgap Semiconductor SiC for Power Devices," *Power Semiconductor Devices and ICs, 2000. Proceedings. The 12th International Symposium on* , vol., no., pp.3,9, 2000

[14]Polzin, K. A., Martin, A. K., Eskridge, R. H., Kimberlin, A. C., Addona, B. M., Devineni, A. P., Dugal-Whitehead, N. R., and Hallock, A. K., "Summary of 2012 Inductive Pulsed Plasma Thruster Development and Testing Program," NASA/TP-2013-217488, 2013.